COENOSES 10(2-3): 123-131, 1995

FRACTAL BASED METHODS IN ECOLOGY: A REVIEW FOR ANALYSIS AT MULTIPLE SPATIAL SCALES[1]

Glen D. Johnson, Arkady Tempelman and Ganapati P. Patil

Center for Statistical Ecology and Environmental Statistics, Department of Statistics, Penn State University,
University Park PA 16802, USA

Keywords: Fractals, Information Theory, Landscape Ecology, Multiscale Analysis, Spatial Scale.

Abstract. As researchers continue to evaluate fractal-based methods of analysis in ecology, a common theme seems to arise as a valuable application: Estimating the fractal dimension or information dimension over a range of spatial scales can deduce ranges of scale-invariance. We present an updated conceptual and methodological review of these methods, with a particular view for multiscale landscape analysis.

Introduction

Observations of nature, whether of its biological or abiotic components, often reveal very complex patterns that can only be very roughly characterized by methods of euclidean geometry. Upon closer inspection, however, the spatial objects or time-series phenomena being observed reveal an underlying simple form that repeats itself at different scales of observation, thus being *scale-invariant* (used interchangeably here with *self-similarity*). Richardson (1926) noted this with turbulence, which he postulated to consist of a "cascade" of self-similar eddies. Theoretical analysis of self-similarity and cascades in the 1940's led to very accurate descriptions of turbulence in the ocean, the atmosphere and large vessels (Grant, Stewart and Moilliet 1959).

Scale-invariance manifests itself algebraically through power laws. A measure of a set F with measurement unit size δ, is related to δ by the relationship $M_\delta(F) \approx c\delta^{-s}$, where s is effectively a *dimension* of F and c is the 's-dimensional' length of F (see Falconer 1990, chap. 3). For many natural objects, however, s is not an integer and therefore F can not be characterized as euclidean. This was observed by Korcak (1938) when parameterizing the size distribution of islands in the Aegean Sea, and by Richardson (1961) when measuring the lengths of coastlines and other land frontiers.

Natural time series phenomena may also exhibit power law relations where the exponent is not what is intuitively expected. Consider the variations in annual cumulative discharge of a river. Since this is dominated by the weather, one may expect annual discharges to be independent (white noise) or to have Markovian dependence at most. As shown by Feller (1951), the range in annual discharges over d years, $R(d)$, would then vary with $d^{1/2}$. However, for the Nile River, Hurst (1951) observed that $R(d)$ varied with d according to $d^{0.9}$. Mandelbrot and Wallis (1969) further discovered that other rivers exhibited exponents between 0.5 and 0.9. By allowing $R(d)$ to vary as $R(d) \approx d^H$, where $0 \leq H \leq 1$, Mandelbrot and Van Ness (1968) proposed that we observe a *fractional* brownian function whenever $H \neq 1/2$.

Mandelbrot (1983) shows that many natural objects are more accurately characterized by mathematical objects that exhibit extreme complexity of shape such as the Koch Curve for defining natural boundaries, the Koch Snowflake for defining areas, and variations of the Cantor Set for defining the size distributions of objects. Such mathematical sets result from recursive iteration of a basic geometric form, thus resulting in a complex structure that is self-similar regardless of measurement scale. Figure 1 shows, for example, the result of the first three iterations of constructing a Koch curve. As the number of iterations goes to infinity, the resulting curve is non-differentiable anywhere and its length goes to infinity. Actually, it is the random counterparts of these sets that more accurately represent natural objects. For example, Figure 2 shows the first three iterations of constructing a random Koch curve which comes closer to mimicking the edge of a lake or forest.

Unlike euclidean objects, these sets are characterized by having a Hausdorf dimension that strictly exceeds their topological dimension and is less than the euclidean dimension of the euclidean space within which the set is embedded. While these sets were deciphered in the late nineteenth and

---

[1] Prepared with partial support from the Statistical Analysis and Computing Branch, Environmental Statistics and Information Division, Office of Policy, Planning, and Evaluation, United States Environmental Protection Agency, Washington, DC under a Cooperative Agreement Number CR-821531. The contents have not been subjected to Agency review and therefore do not necessarily reflect the views of the Agency and no official endorsement should be inferred.

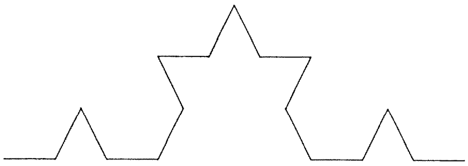

Figure 1. Deterministic Koch curve, after three iterations.

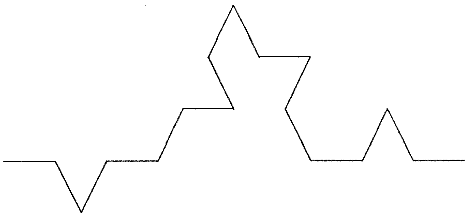

Figure 2. Random Koch curve, after three iterations. The direction of each new triangle was chosen by flipping a coin.

early twentieth century, Mandelbrot (1983) later coined the word *fractals* for collectively defining these entities, where a fractal is characterized by its fractal dimension, which is basically the computable equivalent of its Hausdorf dimension.

While a true fractal is an infinite mathematical set, natural objects are finite, being limited by some fundamental building block, even if it is atomic. Nevertheless, fractal geometry provides a more realistic characterization of the geometry of naturally occurring objects when compared to classical euclidean geometry. This is because, when unconstrained by human manipulation, natural objects are the result of iterative, diffusive growth that results in highly irregular shapes, although the same shape may appear at different scales of observation. Fractal geometry also arises from the need of living organisms to economize space, such as for maximizing the surface area of the digestive and respiratory systems that are constrained by a small volume.

Applications of fractal-based analysis in ecology have been reviewed by Sugihara (1982), Frontier (1987), Milne (1988), Sugihara and May (1990), Hastings and Sugihara (1993), Kenkel and Walker (1993) and Maurer (1994). Cautions are in order, however, such as by Simberloff, et al. (1987) who warn against treating an observed phenomenon as a fractal simply because a linear log-log relationship is observed; furthermore, if a power law relationship is construed as a fractal, this will only be of value if it offers some mechanistic or causal interpretation. Meanwhile, new applications continue to arise.

We present an updated review of different conceptual approaches, along with some historical and recent applications. Our primary motivation is for identifying tools for multiscale landscape level ecological analyses.

Edge Complexity

Consider measuring the length of an irregular edge by adding the number of equal-length measuring rods placed end-to-end from one terminus to the other, where even the smallest practical measuring rods can not resolve all of the edge's curvature. If the curvature pattern is scale invariant, then the resulting length L from using a measuring rod of size (length) δ will change with δ according to the following relationship:

$$L_\delta = k\left(\frac{1}{\delta}\right)^\beta . \qquad (1)$$

Therefore, if $\delta_i < \delta_j$, then $L_{\delta_i} > L_{\delta_j}$, and this change in length is reflected by the scaling exponent β since

$$\frac{L_{\delta_i}}{L_{\delta_j}} = \left(\frac{\delta_j}{\delta_i}\right)^\beta . \qquad (2)$$

When the edge is a fractal, then $\beta = D - 1$, where D is the fractal dimension of the edge (Mandelbrot, 1983).

Note that for the Koch Curve, where each iteration of it's construction corresponds to a 1/3 reduction in δ and a corresponding 4/3 increase in L, then D=log(4)/log(3) ≈ 1.2619.

Coastlines

Using measuring lengths of δ = 10 to 1000 kilometers, Richardson (1961) estimated the lengths of various coastlines and geographic borders, observing very linear relationships between the $\log_{10}(L)$ and $\log_{10}(\delta)$. These results were noticed by Mandelbrot (1983), who related them to Equation 1 and obtained estimates of D that all turned out to be between 1 and 2, being approximately 1.25. This is very close to the fractal dimension of a Koch Curve, as noted above, indicating that coastlines and land frontiers are well characterized by the (random) Koch Curve.

Coral reefs

Bradbury, Reichlet and Green (1984) characterized the fractal dimension of the boundaries of features in an Australian coral reef, where they performed a rolling regression of the log (L) versus log (δ) and found that estimates of D were generally constant over certain ranges of scale δ, but exhibited changes at particular break points.

They found that $D \approx 1.1$ for $\delta \approx$ 10 cm, then declined to $D \approx 1.05$ for δ = 20 cm to 200 cm, followed by a sharp rise to $D \approx 1.15$ for δ = 5 m to 10 m. Since D is reported to be quite constant within each scale range, this suggests that scale invariant phenomena are observed within each range.

As it turned out, the measurement scale ranges that revealed relatively constant fractal dimensions do correspond with the scales of major reef structures. The anatomical features within individual coral colonies, such as branches and convolutions, are detectable at 10 cm measurement scale, while the 20 cm to 200 cm scale corresponds to the size range of whole adult colonies, and 5 m to 10 m corresponds to major geomorphological (abiotic) features.

Area Complexity

Equations 1 and 2 can readily be extended to *areas* or *patches* that are defined by fractal edges that form a closed loop. In this case, δ refers to the length of the side of a square box, such that an area is covered by a tesselation of these boxes. The minimum number of boxes of size δ that intercept the area represents a δ-cover of the area (Sugihara and May, 1990). For a given δ, the minimum number of boxes that intercept the area is counted. After repeating this exercise with other δ-coverings, if the log (number of boxes) is linearly related to log (δ), then the same form as Equation 1 is applicable. The area measured in this way, A_δ, can be expressed as $A_\delta \propto a\delta^{2-D_b}$, where D_b is often called the box dimension.

If the patch perimeter is characterized by Equation 1, then we can designate the perimeter length as $P_\delta = p\,(1/\delta)^\beta$, using a "measuring rod" of length δ. Therefore, the perimeter scaling exponent β is related to the box dimension by

$$D_b = 2 + \beta\left(\frac{\log(A_\delta) - \log(a)}{\log(P_\delta) - \log(p)}\right) \tag{3}$$

Since $\log(A_\delta) < \log(a)$, the dimension D_b decreases as β increases, reflecting increasing convolutedness or jaggedness of the perimeter.

Geographic range of breeding birds

Maurer (1994) observed that the log(number of boxes) is very linearly related to log (δ) for the geographic range of several Sparrow species in the United States. Using Equation 1, he obtained the following box dimensions: $D_b = 1.57$ for Henslow's Sparrow and $D_b = 1.62$ for Baird's Sparrow which had similar extents of their home ranges, and $D_b = 1.72$ for the Grasshopper Sparrow, which had a much larger home range than the other two Sparrows.

For these particular bird species, the Grasshopper Sparrow appears to be the least prone to extinction in the United States because it not only has the largest home range extent, but also reveals the least convoluted, and subsequently greater space filling, range boundary. Of the two Sparrows that have smaller home ranges, Henslow's Sparrow appears to be more susceptible to extinction because its home range boundary is the most convoluted, reflecting greater population fragmentation.

Arthropod habitat space on vegetation

Using photographs of plants, Morse et al. (1985) used the same box-counting method described above to characterize the fractal dimension of plant outlines in order to characterize the habitat space for arthropods that live on plants. The resulting values ranged from $D = 1.28$ to $D = 1.79$.

These authors speculated that if animals utilize their environment in proportion to body length, then apparent habitat space can be computed by Equation 1, where animal length l is substituted for δ. Supposing that population densities are approximately proportional to the reciprocal of individual rates of resource utilization, then if resource per individual is proportional to the 0.75 power of body weight (a known allometric relation that may have its own fractal interpretation), it follows that population density N scales as $(l^3)^{-0.75}$. Therefore, a 10-fold decrease in body length results in a $(10^3)^{0.75} = 178$-fold increase in the density of individuals. This result can be combined with the expected increase in available surface area that is a function of the surface fractal dimension. Since the surface fractal dimension is not a straightforward calculation, Morse et al. (1985) obtain heuristic upper and lower bounds of the expected increase in surface area for an order of magnitude decrease in ruler length (body length), such that the range is 3.16 to 10.0.

Subsequently, for an order-of-magnitude decrease in body length, the predicted increase in animal numbers is 178(3.16) = 560-fold to 178(10) = 1,780 fold. Interestingly, data reported by these authors for the actual arthropod numbers (mainly insects) on vegetation from a wide variety of locations and vegetation types do fall within these predicted values.

Area-Perimeter Relationships

Equation 3 expresses the relationship between the measured area and perimeter of a patch for a fixed measurement scale δ. When assessing many patches (or islands) whose perimeters are of the same fractal dimension, another way to estimate this dimension is to measure the area and perimeter of many patches, using a single fixed measurement scale δ. As shown by Hastings and Sugihara (1993, pp. 48-50), when the perimeter p and area A are measured on a collection of patches having the same fractal dimension, the inherent scale invariance amongst these patches implies the power law relationship

$$p = k\,A^E \,, \tag{4}$$

where E is equivalent to one half of the fractal dimension of the patch perimeters, $E = D/2$.

Clouds and rain areas

Lovejoy (1982) analyzed infrared pictures of clouds over the Indian Ocean with a resolution of 4.8 by 4.8 km, and radar pictures of tropical rain areas with a resolution of 1 by 1 km. Plotting the $\log_{10}$ (area in km^2) against $\log_{10}$ (perimeter in km), he discovered a very linear relationship over an area range of six orders of magnitude and a perimeter range of nearly five orders of magnitude. The cloud and rain area data sets revealed equivalent slopes with a corresponding estimate of $D \approx 1.35$.

The equivalent fractal dimensions allow the combination of both data sets for substantially increasing the degrees of freedom in estimating D. For a fractal object of dimension D, a perimeter L_1 that is measured by a smaller measurement scale is greater than a perimeter L_2 that is measured by a coarser scale by a factor of $(L_1/L_2)^{1-D}$. Therefore, Lovejoy multiplied the cloud perimeters by a factor of $(1/4.8)^{-0.35} = 1.73$, and observed that both data sets fell on the same straight line.

Landscape patterns: distinguishing the natural from the disturbed

Krummel et al. (1987) applied the perimeter-area method to evaluate the fractal dimension D of deciduous forest patches in southern Mississippi and central Louisiana, where much of the area had been converted to agricultural land over the previous 30 years. Using a measurement scale of 10m resolution, these authors estimated D as a function of area by performing a rolling regression of log(perimeter) versus log(area). The first estimate of D was obtained from regressing the 200 smallest patches, with successive regressions formed by removing the smallest and adding the next largest patch.

Their results showed that D varied between 1.1 and 1.2 for areas up to around 60 ha, after which D rose sharply and varied between 1.35 and 1.45 for areas greater than 70 ha. Regressions on the 200 smallest patches that were less than 55.7 ha yielded an estimate of $D=1.20 \pm 0.02$ ($R^2=0.78$), and regressions on the 200 largest patches that exceeded 100.4 ha yielded $D=1.52 \pm 0.02$ ($R^2=0.90$).

These results were interpreted to indicate that human disturbances predominate at smaller spatial scales where forest perimeter dimensions are closer to 1.0, the euclidean dimension of a straight line. Meanwhile, forest patch dynamics on larger scales appear to be governed more by natural processes, thus leading to more complex fractal edges. Hastings and Sugihara (1993) point out that the dimension of 1.52 is close to that of islands $(x,y) : z\ (x,y) \geq 0$ formed by a Brownian function $z=f(x,y)$.

Patch-Size Distributions

When parameterizing the size distribution of islands in the Aegean Sea, Korcak (1938) observed an empirical power-law relationship where the number of islands greater than size a follows a hyperbolic distribution such that

$$N(A > a) = ka^{-B}\,, \tag{5}$$

where k and B are estimated from log/log regression. Mandelbrot (1983) noted that B always exceeds 1/2 and shows that Equation 5 is the counterpart of the distribution of gap lengths in a Cantor dust (a true fractal). Basically, when islands or patches are delineated by boundaries having the same fractal dimension, then by scale-invariance Equation 5 holds true and B can be shown to equal $D/2$ ($0 \leq B \leq 1$) (Hastings and Sugihara, 1993).

Vegetation patches in the Okefenokee Swamp

Hastings et al. (1982) noticed that the size (area) distribution of vegetation patches in the Okefenokee Swamp was similar to the observations Korcak made on islands in the Aegean Sea. Using log/log regression to estimate the parameters of Equation 5, these investigators evaluated different areas of both Cypress and Broadleaf forests within the swamp. Noting that B measures the number of small patches relative to the number of large ones, they observed that Cypress appeared ''patchier'' than the Broadleaf forest, suggesting that Cypress is less persistent. Note that Cypress grows in water on peat, which can be fragmented by fires during severe drought, while broadleaf trees grow on islands within the swamp (Loehle, C., 1995; personal communication). Subsequently, one may expect the observed patchiness that was characterized by fractal analysis in this study.

Hastings and Sugihara (1993, p. 122) further note that the exponent B associated with a given type of vegetation (1) decreases with the stage of ecological succession since late successional patterns are less patchy than earlier successional stages; and (2) decreases with increasing persistence of the vegetation type.

Variogram Analysis

As noted in the introduction, time series phenomena may behave as a fractional brownian function. This same concept applies to spatial analysis where some feature is measured on plots across a surface or points along a transect.

In a similar fashion as fractal time series, the autocorrelation structure of a spatial random variable, Z, can be described by its semivariance such that

$$2\gamma(h) = E\,[\,Z_{x+h} - Z_x]^2 = h^{2H}\ , \tag{6}$$

where Z_{x+h} and Z_x are values of a random variable separated by a spatial lag h. As defined by Mandelbrot (1983, p.353), H can vary between zero and one, where $H=1/2$ corresponds to no spatial autocorrelation for any lag h. For $H > 1/2$, the spatial autocorrelation is positive, resulting in an increasingly smooth response across space as H increases above 1/2. Likewise, for $H < 1/2$, the spatial autocorrelation is negative, resulting in increasing jaggedness across space as H decreases below zero.

Estimated values of H can be obtained from the slope of linear regions of a log-log plot of Equation 6, where $\gamma(h)$ is estimated from the experimental variogram,

$$\hat{\gamma}(h) = \frac{1}{2N(h)} \sum_{i=1}^{N(h)} (z_{x+h} - z_x)^2 \tag{7}$$

with $N(h)$ being the number of pairs of measured points (z_{x+h}, z_x), separated by euclidean distance h.

Soil variation

Burrough (1983) notes that the fractal dimension of a fractional brownian response from a transect is related to the exponent H by $D=2-H$. Therefore, the slope of a linear region of the log-log plot of 6 equals $m=2H=4-2D$. By this method, Burrough (1983) estimated D for various soil properties which all revealed dimensions between 1.5 and 2.0, indicating that these properties are all negatively autocorrelated ($H < 1/2$). This was not the case, however, for topographic height which revealed D=1.3, indicating that it is positively autocorrelated as expected with a smoother response. While self-similarity was not equivalent amongst all soil scales, as with an ideal fractal, the observed variograms and corresponding fractal dimensions indicated that high variation does persist as the scales of soil structure become very small.

Vegetation variation

He et al. (1994) applied variogram analysis to a forest in order to estimate the fractal dimension of different measurement "response surfaces". For each of three measurements (tree richness, density and Shannon diversity), a surface was defined by tessellating a rectangular experimental forest by equal-sized cells, followed by obtaining a measurement in each cell. This was then repeated for different measurement scales (cell sizes). The fractal dimension for each measurement surface, which lies between 2 and 3, is related to the exponent H by $D=3-H$. The estimated slope of a linear region of a log-log plot of the semivariogram then equals $m=2H=6-2D$.

All surfaces appeared to be generally isotropic, especially at the smaller measurement scales. The fractal dimension for all three measurements were near D=3 at the smallest measurement scale and generally decreased as the measurement scale increased, thus reflecting an increasing smoothing effect of larger cell sizes in the tesselation. Such observations highlight the need to consider that different measurement scales can give rise to different spatial patterns over the same geographic area.

Spatial patterns of vegetation have also been quantified by estimating the fractal dimension from variograms obtained from linear transects (Palmer 1988), as with Burrough's soil study; however, the location and orientation of transects has been shown to be a significant source of variability along with changing the measurement scale (LeDuc et al. 1994). Therefore, one must consider these factors when designing a study for estimating the fractal dimension of spatial distributions of vegetation or other variables.

Information Theoretic Applications

As multivariate systems, ecosystems are often characterized by information statistics which are empirical versions of Shannon's entropy, described as

$$H = -\sum_{i=1}^{s} f_i \log f_i \qquad (8)$$

for s components, each occurring with relative frequency f_i such that $\sum_{i=1}^{s} f_i = 1$. While this index has been used extensively for characterizing species diversity, it also provides the basis for entropy-based landscape metrics (O'Neill, et al., 1988). For both of these very different applications, fractal concepts may play a role, as discussed in the following examples.

Species diversity

When species diversity of a community or a sample is expressed by the Shannon statistic, then diversity is expressed as a product of community evenness ($J=H/H_{max}$) and species richness, expressed as $\log_2(s)$ for s species, since $H_{max} = \log_2(s)$. Frontier (1987) points out that diversity H is the mathematical expectation of $-\log_2 f_i$ when calculated over the s species. Using Frontier's terminology, $H = E[-\log_2 f_i\,] = \log_2(A)$, where A is the number of species that would yield the same diversity index if all species were equifrequent. Evenness is then expressed as $J=\log_2(A)/\log_2(s)$ which takes the form of a dimension when reexpressed as $A=s^J$. Here we see how the diversity-equivalent number A of equifrequent species increases as the real number of species s increases, for a given evenness value J.

Landscape diversity

The methods for characterizing landscape patterns that were previously mentioned, namely the perimeter-area, box counting and patch size distribution methods, all apply to a binary classification of landscapes where boundaries are sharply defined. A more natural realization of a landscape includes multiple land cover types where boundaries have fuzzier distinctions (Loehle and Wien, 1994). In order to capture this detail, information theoretic approaches appear to be more appropriate.

When a landscape is tessellated into $M(\delta)$ equal sized cells (pixels), where each cell has a side of length δ, we can calculate the Shannon entropy as in Equation 8 if we can transform the values in each cell to a probability space. In other words, each cell takes a value p_i such that $0 \leq p_i \leq 1$ and $\sum_{i=1}^{M(\delta)} p_i = 1$.

As an example, consider the diagram in Figure 3 where a point process is overlaid with a tesselation of equal sized cells. A p value can be obtained for each cell by

$$p_i = \frac{n_i}{\sum_{i=1}^{M(\delta)} n_i}, \qquad (9)$$

where n_i equals the number of points falling within the ith cell. By Equation 8, using natural logarithms, entropy for the point set in Figure 3 equals $3.9995 \approx 4.00$. For comparison, the maximum entropy is obtained when the points are uniformly distributed (each cell contains an equal number of points), which implies $H(\delta)_{max} = \ln(M(\delta)) = \ln(400) = 5.99$; and minimum entropy is obtained when all points fall in only one cell, which implies $H(\delta)_{min} = 0$. If this exercise is repeated for different cell sizes (δ), ranges of δ which reveal a linear scaling of $H(\delta)$ such that

$$H(\delta) = H_0 - \sigma \ln(\delta)\,, \qquad (10)$$

reveal scaling ranges of self-similarity. Here, σ is called the information dimension which is a lower bound of the Hausdorf (fractal) dimension (Grassberger and Procaccia 1983).

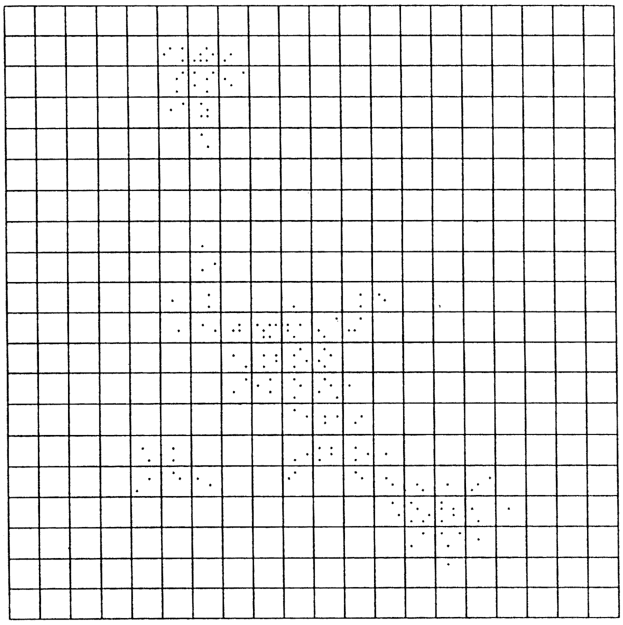

Figure 3. Example of a point process embedded in the euclidean plane, overlaid with a regular grid of equal size cells.

An equivalent approach for analyzing ecological time series is discussed by Maurer (1994, pp. 100 - 110).

Loehle and Wien (1994) have estimated the information dimension of a landscape over several measurement scales (δ), using an innovative transformation of pixelized data to probability space. Starting with six classified forest types in a portion of the Hatchie River watershed in western Tennessee, these authors ordinated the forest types with respect to tree species importance values. Each pixel in their image was then assigned ordination scores according to the primary ordination axes. These scores were then transformed to probability space ($0 \leq p_i \leq 1$ for $i = 1, ..., M(\delta)$ pixels) such that pixels with the mean ordination value have $p_i = 0$, and all non-zero p_i values are a measure of the deviation from the mean. The information dimension was then estimated between discrete measurement scales as

$$d_I(\varepsilon) = \frac{\sum_{i=1}^{K(\varepsilon)} P_i \log P_i - \sum_{i=1}^{K(\gamma)} P_j \log P_j}{\log[1/\varepsilon] - \log[1/\gamma]} \tag{11}$$

where $K(\varepsilon)$ and $K(\gamma)$ are the number of pixels at each measurement scale such that $\varepsilon < \gamma$.

With non-forest areas assigned the mean ordination value of zero, d_I varied from 2.654 at the finest measurement scale to 1.344 at the second coarsest scale, while five scales in-between revealed d_I that only varied between about 1.85 and 1.95. These results indicate that observed forest landscape diversity is very high at small measurement scales (pixel sizes), while the larger measurement scales reveal lower diversity that corresponds to greater fragmentation. Furthermore, statistical self-similarity was revealed over five measurement scales which correspond to a large spatial range.

For comparison, a binary map was created by assigning a value of 1 to forested pixels and 0 to non-forested pixels. The resulting information dimension for the binary map was approximately 1.85 over all measurement scales, thus revealing universal self-similarity. These results show how a simple binary classification of a landscape can obscure valuable information about scale dependence.

In another application of information theory for assessing landscape diversity, Costanza and Maxwell (1994) measured the predictability of categorizing the land use associated with pixels on landscape images. These authors evaluated what they call auto-predictability (Pa) and cross-predictability (Pc), where Pa is the ability to predict the category of a pixel based on the categories of adjacent pixels, akin to a measure of contagion (O'Neill et al. 1988), and Pc is the ability to predict the category of a pixel based on values of the same pixel in other scenes. Following Colwell (1974), predictability is basically the compliment of conditional uncertainty, which is in turn measured as entropy in the form of Equation 8.

Using digitized land use maps from Maryland and southern Florida, the authors investigated Pa and Pc over a range of five different measurement scales. Starting with the "floor" resolution, coarser scales were obtained by grouping four pixels into one and assigning the land use category to the new larger pixel according to the category of the smaller pixel that was in the northwest corner. When the ln(P) was plotted against ln(r), where r equals the number of cells per unit area, an increasing linear relation was observed for Pa and a decreasing linear relation was observed for Pc. The authors felt that these linear trends reflect ''fractal-like'' *self-similar* measures, which may allow conversion of P measured at one scale to another scale (resolution). To this end, they modeled their results by regressing ln(P) against ln(r), claiming that the slope equals $1\text{-}D_p$, where D_p is a fractal predictability dimension.

While auto-predictability and cross-predictability are potentially valuable indices of spatial dynamics, extending the observed linear scaling to a fractal dimension still requires a theoretical foundation. Interpreting the scaling exponent as $1\text{-}D$ may not be appropriate, since this relates to a self-similar geometric shape when the overall size of the shape is related directly to measurement scale ($L=k\delta^{1\text{-}D}$). Since resolution, r, is the number of pixels per unit area, then $r \propto 1/\delta$ as in Equation 1. Therefore, even if a model for geometric self-similarity is applicable to the information measurements of predictability, the slope would be $D\text{-}1$, not the converse.

Multifractals and Conditional Fractal Distributions

When the attractor of a dynamical system is manifested as a distribution of points, Hentschel and Procaccia (1983) show that an infinite number of generalized dimensions exist for characterizing such an attractor. The generalized dimension of an attractor is then defined as

$$D_q = \frac{1}{(q-1)} \lim_{\delta \to 0} \frac{\log \sum_{i=1}^{M(\delta)} p_i^q}{\log(\delta)}\ , \tag{12}$$

where δ, p_i and $M(\delta)$ are as defined in the previous section, and q is any real number such that $q > 0$ and $q \neq 1$.

Hentschel and Procaccia (1983) show that $\lim_{q \to 0} D_q =$ the Hausdorf similarity dimension D of a geometric shape, which is the *classical* fractal dimension we discussed in earlier sections, and $\lim_{q \to 1} D_q =$ the information dimension, σ, as we discussed in the last section. D_2 equals the correlation dimension, ν, which is defined by $C(\delta) \cong \delta^{\nu}$, where $C(\delta)$ is the number of pairs of points whose distance $| X_i - X_j |$ is less than δ. The authors further prove that $\nu \leq \sigma \leq D$, with equality only occurring when the points are uniformly distributed, meaning that $p_i = p_j$ for all $i \neq j$.

For measurements of natural objects, Scheuring and Riedi (1994) indicate that D_q is estimable as the slope of a linear region of a plot of $(q-1)^{-1} \log \sum_{i=1}^{M(\delta)} p_i^q$ versus $\log(\delta)$. The authors further extended the application of multifractals for analyzing landscapes that consist of many different point sets, such as soil moisture, vegetation cover, etc.

Letting $p_i(l_j \mid l_1,\ldots,l_m)$ be the proportion of type j points in the ith cell, given that at least one point from each of the sets $l_1, \ldots, l_m$ also occurs in cell i, Equation 12 can be reexpressed as

$$D_q(l_j \mid l_1,\ldots,l_m) = \frac{1}{(q-1)} \lim_{\delta \to 0} \frac{\log \sum_{i=1}^{M(\delta, l_1,\ldots,l_m)} (p_i(l_j \mid l_1,\ldots,l_m))^q}{\log(\delta)}\ , \tag{13}$$

for $j=1, \ldots, m$ different types of points and $M(\delta, l_1, \ldots, l_\mathrm{m})$ cells.

Scheuring and Riedi (1994) simulated two different point patterns for each of two competing hypothetical species and computed the multifractal moments of these four point patterns. Their results show that the independent multifractal moments, based on Equation 12, were nearly identical between the two patterns within each species; however, when the estimated multifractal moments for one species were conditional on the pattern of the other species, based on Equation 13, much greater differences were revealed between the two patterns within each species. These results indicate that estimates of conditional multifractal dimensions may provide a tool for assessing the dependence of the pattern of one patch type on the patterns of other patch types.

This methodology is conceptually similar to that proposed by Milne (1992), who presents a model for the cooccurrence of fractally distributed species. For a grid consisting of δ-sized cells, the number of cells occupied by a particular patch type (species or resource) equals $N(\delta) = C\delta^{-D_g}$, where D_g is the grid fractal dimension for this particular patch type. The proportion of total grid cells occupied by this patch type is then

$$\mathrm{prop}(\delta) = \frac{C\delta^{-D_g}}{(E/\delta)^2}, \tag{14}$$

where the denominator is the number of cells of size δ^2 over a square map with E cells along one side. If all patch types are characterized by fractal distributions that are independent of each other, then a ''neutral'' model that predicts the proportion of the landscape occupied by s patches is

$$A(\delta) = \prod_{i=1}^{s} \frac{C_i \delta^{-D(i)_g}}{B\delta^2} \tag{15}$$

where each of the s independent patches has a grid fractal dimension of $D(i)_g$. B in the denominator is a constant that varies with extent such that $B\delta^2$ is the total grid area. Equation 15 simply follows from the laws of independence.

This neutral model can be extended to a landscape that is constrained by the fractal distribution of a particular patch. Such a conditional neutral model is defined by Milne (1992) as

$$\mathrm{prop}\ (\delta) = \prod_{i=1}^{s} \frac{A_i \delta^{-D(i)_g}}{B\delta^2} \mid \min(C_j \delta^{-D(i)_g}) \tag{16}$$

which defines the proportion of grid cells occupied by the ith patch type measured only in grid cells that are in turn occupied by patch type j whose coverage at scale δ is less than any other of the s patch types. This patch type j may be the most rare species of a group of s species for which a nature reserve is being designed, or it may be a limiting resource.

Stochastic Similarity Dimension and Entropy

The usage of informational characteristics in multiscale analysis can be justified by the study of the dimension of self-similar stochastic processes. The simplest case of such a process can be described formally as follows.

Let A be a set in m-dimensional Euclidean space, N a positive integer and L a subset of cardinality K of the set 1,...,N. Assume $A = \cup_{i_1=1}^{N} A_{i_1}$ where A_{i_1} are disjoint and geometrically similar to A. Let $A_{i_1} = \cup_{j_2=1}^{N} A_{i_1 j_2}$ where $A_{i_1 j_2}$ are disjoint and geometrically similar to A, and so on. At the nth step of this procedure, we come to a partition of A by disjoint sets $A_{i_1,\ldots,i_n}$ that are similar to A. We assume that if $\{i_1,\ldots,i_n\} \in L$ then, in $A_{i_1},\ldots$in , our system may be in one of the states $S_1,\ldots,S_M$, and the probability that the system is in $A_{i_1,\ldots,i_n,i_{n+1}}$ in the state S_l, given that it is in the state S_k in the set $A_{i_1,\ldots,i_n}$, is equal to P_{kl}. Such a system is said to be *stochastically self-similar* if, in addition, the probability P_l of being in state S_l is the same for all sets $A_{i_1,\ldots,i_n}$ if $\{i_1,\ldots,i_n\} \in L$ and $1 \leq l \leq M$.

Let C be the "carrier" of our system, meaning that the set of all points $\{a\} \in A$ such that $\{a\} = \cap_{n=1}^{\infty} A_{i_1,\ldots,i_n}$ where $\{i_1,\ldots,i_n\} \in L$. Now consider that a self-similar process can be viewed as a stationary Markov Chain. An argument similar to one used in Pesin and Tempelman (1995) allows us to prove that the correlation dimension of the associated shift dynamical system turns out to be equal to

$$d = \frac{mH_p}{\log N} + \frac{m\log K}{\log N} \tag{17}$$

$$= d_p + d_c \tag{18}$$

where d_c is the Hausdorf dimension of the carrier C (which coincides with Mandelbrot's similarity dimension). H_p, defined as

$$H_p = -\sum_{k=1}^{M} P_k \sum_{l=1}^{M} P_{kl} \log P_{kl}, \tag{19}$$

is the conditional entropy with conditional probabilities P_{kl}. This argument shows that, in a stochastically self-similar system, the conditional entropy H_p is closely related to the correlation dimension of the process.

The quantity $d = d_p + d_c$ can be considered as the "stochastic similarity dimension", where d_c is the component of deterministic origin and d_p is the component of stochastic origin due to the random nature of the spatial process, as specified by the conditional entropy H_p.

We are currently studying such processes and their applications to multiscale spatial analysis. Our primary database for empirical studies consists of digital land cover images of the state of Pennsylvania which contains 256 categories that are based on LANDSAT thematic mapper imagery which provides a floor resolution of 30 meter pixels.

Summary

For all the excitement and disappointments, fractal-based analysis appears to have some strong practical applications for performing landscape level analyses over different measurement scales (i.e., digitized polygons) and different landscape scales (i. e., patch sizes ranging from woodlots to mountainsides). Of primary importance is the identification of scaling ranges that encompass scale invariance.

On one hand, this is necessary for comparing spatial patterns that may be assessed at different measurement scales, such as with 30 meter resolution LANDSAT TM images versus 20 meter resolution SPOT images. If the different measurement scales are within a range of scale invariance, these multiscale measurements may be directly comparable.

On the other hand, understanding landscape ecology requires the identification of different spatial scales that reflect different underlying processes. For example, observed vegetation patterns may be defined by soil patterns at one scale and geological patterns at another scale. The association between species or between species and resources at one scale may appear competitive, while the association appears mutualistic at another scale.

Delineation of scale-invariant measurement ranges or size ranges of statistically self-similar objects need to be based on quantitative decision-making that controls type 1 and type 2 error rates. Thus far, scaling ranges have been delineated from "eyeballing" breaks in the linearity of log-log plots or in changes of fractal dimension estimates when plotted over different scales. If such estimates are simply regression estimators, then testing for equivalence of slopes may be appropriate. Most studies so far have not accounted for the different sources of variability of either fractal dimension or information dimension estimators, a concern raised earlier by Kenkel and Walker (1993). An empirical study for a particular area was performed by LeDuc et al. (1994); however, more of this is necessary. Furthermore, in a very recent paper, Loehle and Li (1995) point out that the assumptions underlying regression analysis are not satisfied when using regression to estimate a fractal dimension. Such concern lends support for working with the discrete-step information dimension (Equation 11) that was applied by Loehle and Wien (1994).

Information theoretic approaches appear to be most capable of capturing the detail associated with multiple patch types that have fuzzy boundaries, thus allowing for more realistic characterizations of actual landscapes. Extending these notions to conditional fractal distributions may further allow quantification of the degree of association (positive or negative) between different entities that are distributed in a fractal manner. Such entities include physical features like mosaics of soil, geological formations and moisture, as well as biological populations and communities.

Viewing landscape transitions across multiple spatial scales as a Markov dynamical process, we may be able to estimate a stochastic similarity dimension between any two scaling steps. Such a dimension incorporates a probabilistic component that quantifies the conditional entropy as we move from one scale to another. Hopefully, such research will result in methods that may allow landscape ecologists to (1) quantify the influence of one scale on another, (2) test hypotheses of equivalent scaling domains and (3) provide a multiscale measurement that can be used for quantitatively comparing landscapes.

Acknowledgements. We are very grateful to our colleagues Robert Hengeveld, Bai-Lian Li, Craig Loehle, Wayne Myers and George Sugihara and for their very constructive and supportive reviews of this manuscript.

References

Bradbury, R.H., Reichlet, R.E. and Green, D.G. 1984. Fractals in ecology: methods and interpretation. Marine Ecol. Prog. Ser., 14:295-296.

Burrough, P.A. 1983. Multiscale sources of spatial variation in soil. I. The application of fractal concepts to nested levels of soil variation. J. Soil Sci., 34:577-597.

Colwell, R.K. 1974. Predictability, constancy, and contingency of periodic phenomena. Ecology, 55:1148-1153.

Costanza, R. and Maxwell, T. 1994. Resolution and predictability: an approach to the scaling problem. Landscape Ecology, 9(1):47-57.

Falconer, K. 1990. Fractal Geometry, Mathematical Foundations and Applications . John Wiley, Chichester.

Feller, W. 1951. The asymptotic distribution of the range of sums of independent random variables. Ann. Math. Stat., 22:427-432.

Frontier, S. 1987. Applications of fractal theory to ecology. in Legendre, P. and Legendre, L. (eds.), Developments in Numerical Ecology . NATO ASI Series, Vol. G14, Springer-Verlag, Berlin, pp. 335-378.

Grant, H.L., Stewart, R.W. and Moilliet, A. 1959. Turbulence spectra from a tidal channel. J. Fluid Mechanics, 12:241-268.

Grassberger, P. and Procaccia, I. 1983. Measuring the strangeness of strange attractors. Physica, 9D:189-208.

Hastings, H.M., Pekelney, R. Monticciolo, R. vun Kannon, D. and del Monte, D. 1982. Time scales, persistence and patchiness. Biosystems, 15:281-289.

Hastings, H.M. and Sugihara, G. 1993. Fractals: A User's Guide for the Natural Sciences . Oxford University Press, Oxford. 235 pp.

He, F., LeGendre, P., Bellehumeur, C. and LaFrankie, J.V. 1994. Diversity patterns and spatial scale: a study of a tropical rain forest of Malaysia. Environ. Ecol. Stat., 1:265-286.

Hentschel, H.G.E. and Procaccia, I. 1983. The infinite number of generalized dimensions of fractals and strange attractors. Physica, 8D:435-444.

Kenkel, N. C. and Walker, D. J. 1993. Fractals and ecology. Abstracta Botanica 17:53-70.

Korcak, J. 1938. Deux types fondamentaux de distribution statistique. Bulletin de l'Institut International de Statistique, III:295-299.

Krummel, J.R., Gardner, R.H., Sugihara, G., O'Neill, R.V. and Coleman, P.R. 1987. Landscape patterns in a disturbed environment. Oikos, 48:321-324.

LeDuc, A., Prairie, Y.T. and Bergeron, Y. 1994. Fractal dimension estimates of a fragmented landscape: sources of variability. Landscape Ecology, 9(4):279-286.

Loehle, C. and Li, B. 1995. Statistical properties of ecological and geologic fractals. Ecol. Modeling (in press).

Loehle, C. and Wein, G. 1994. Landscape habitat diversity: a multiscale information theory approach. Ecol. Modeling, 73:311-329.

Lovejoy, S. 1982. Area-perimeter relation for rain and cloud areas. Science, 216(9):185-187.

Maurer, B.A. 1994. Geographical Population Analysis: Tools for the Analysis of Biodiversity . Blackwell Scientific, London, 130 pp.

Mandelbrot, B. B. 1983. The Fractal Geometry of Nature . W.H. Freeman and Co., New York, 468 pp.

Mandelbrot, B. B. and Van Ness, J.W. 1968. Fractal brownian motions, fractional noises and applications. SIAM Review, 10:422.

Mandelbrot, B. B. and Wallis, J.R. 1969. Some long-run properties of geophysical records. Water Resources Research, 5:321-340.

Milne, B.T. 1988. Measuring the fractal geometry of landscapes. Appl. Math. and Comp., 27:67-79.

Milne, B.T. 1992. Spatial aggregation and neutral models in fractal landscapes. The American Naturalist, 139:32-57.

Morse, D.R., Lawton, J.H., Dodson, M.M., and Williamson, M.H. 1985. Fractal dimension of vegetation and the distribution of arthropod body lengths. Nature, 314:731-733.

O'Neill, R.V., Krummel, J.R., Gardner, R.H., Sugihara, G., Jackson, B., DeAngelis, D.L., Milne, B.T., Turner, M.G., Zygmunt, B., Christensen, S.W., Dale, V.H., and Graham, R.L. 1988. Indices of landscape pattern. Landscape Ecol., 1(3):153-162.

Palmer, M.W. 1988. Fractal geometry: a tool for describing spatial patterns of plant communities. Vegetatio, 75:91-102.

Pesin, Ya and Tempelman, A. 1995. Correlation dimension of measures invariant under group actions. Random and Computational Dynamics, 3(3):137-156.

Richardson, L.F. 1926. Atmospheric diffusion shown on a distance-neighbor graph. Pr. of the Royal Society of London, A, 110:709-737.

Richardson, L.F. 1961. The problem of contiguity: an appendix of statistics of deadly quarrels. General Systems Yearbook, 6:139-187.

Scheuring, I. and Riedi, R.H. 1994. Application of multifractals to the analysis of vegetation pattern. J. Vegetation Sci., 5:489-496.

Simberloff, D., Berthet, P., Boy, V., Cousins, S.H., Fortin, M.J., Goldburg, R., Lefkovitch, L.P., Ripley, B., Scherrer, B., and Tonkyn, D. 1987. Novel statistical analyses in terrestrial animal ecology: dirty data and clean questions. in Legendre, P. and Legendre, L (eds.), Developments in Numerical Ecology . NATO ASI Series, Vol. G14, Springer-Verlag, Berlin, pp. 559-572.

Sugihara, G. 1982. Applications of fractals to the study of landscape pattern. Oak Ridge National Laboratory Technical Memo.

Sugihara, G. and May, R.M. 1990. Applications of fractals in ecology. Trends in Research in Ecol. and Evol., 5(3):79-86.